



HAL
open science

TTBK2 kinase substrate specificity and the impact of spinocerebellar ataxia-causing mutations on expression, activity, localisation and development

Michale Bouskila, Noor Esoof, Laurie Gay, Emily H Fang, Maria Deak, Mike Begley, Lewis C Cantley, Alan Prescott, Kate G. Storey, Dario R Alessi

► **To cite this version:**

Michale Bouskila, Noor Esoof, Laurie Gay, Emily H Fang, Maria Deak, et al.. TTBK2 kinase substrate specificity and the impact of spinocerebellar ataxia-causing mutations on expression, activity, localisation and development. *Biochemical Journal*, 2011, 437 (1), pp.157-167. 10.1042/BJ20110276 . hal-00600763

HAL Id: hal-00600763

<https://hal.science/hal-00600763>

Submitted on 16 Jun 2011

HAL is a multi-disciplinary open access archive for the deposit and dissemination of scientific research documents, whether they are published or not. The documents may come from teaching and research institutions in France or abroad, or from public or private research centers.

L'archive ouverte pluridisciplinaire **HAL**, est destinée au dépôt et à la diffusion de documents scientifiques de niveau recherche, publiés ou non, émanant des établissements d'enseignement et de recherche français ou étrangers, des laboratoires publics ou privés.

TTBK2 kinase substrate specificity and the impact of spinocerebellar ataxia-causing mutations on expression, activity, localisation and development.

Michale Bouskila^{1*}, Noor Esoof¹, Laurie Gay^{1♦}, Emily H. Fang², Maria Deak¹, Mike Begley³, Lewis C. Cantley³, Alan Prescott⁴, Kate G. Storey² and Dario R Alessi¹

1. MRC Protein Phosphorylation Unit, College of Life Sciences, University of Dundee, Dow Street, Dundee DD1 5EH, Scotland UK.
2. Division of Cell and Developmental Biology, College of Life Sciences, University of Dundee, Dow Street, Dundee DD1 5EH, Scotland UK.
3. Department of Systems Biology, Harvard Medical School, Boston, MA 02115, US.
4. Division of Cell Signalling and Immunology, College of Life Sciences, University of Dundee, Dow Street, Dundee DD1 5EH, Scotland UK.

* Current address, Dando, Weiss and Colucci, East Road Cambridge CB1 1BH.

♦ Current address, Trends in Molecular Medicine, 600 Technology Square, Cambridge, MA, USA 02139

Short Title: Impact of spinocerebellar ataxia mutations on TTBK2

Correspondence to DRA (d.r.alessi@dundee.ac.uk)

Accepted Manuscript

Abstract

Mutations that truncate the C-terminal, non-catalytic moiety of the Tau tubulin Kinase 2 (TTBK2) cause the inherited, autosomal dominant inherited spinocerebellar ataxia type 11 (SCA11) movement disorder. In this study we first assess the substrate specificity of TTBK2 and demonstrate that it has an unusual preference for a phosphotyrosine at the +2 position relative to the phosphorylation site. We elaborate a peptide substrate (TTBKtide, RRKDLHDDEEDEAMSIYpA) that can be employed to quantify TTBK2 kinase activity. Through modelling and mutagenesis we identify a putative phosphate priming-groove within the TTBK2 kinase domain. We demonstrate that SCA11 truncating mutations promote TTBK2 protein expression, suppress kinase activity and lead to enhanced nuclear localisation. We generate an SCA11-mutation-carrying knock-in mouse and show that this leads to inhibition of endogenous TTBK2 protein kinase activity. Finally, we find that in homozygosity, the SCA11 mutation causes embryonic lethality at E10. These findings provide the first insights into some of the intrinsic properties of TTBK2 and reveal how SCA11-causing mutations impact on protein expression, catalytic activity, localisation and development. We hope these findings will be helpful for future investigation of the regulation and function of TTBK2 and its role in SCA11.

Introduction

Recent studies have revealed that mutations within the Tau tubulin Kinase 2 (TTBK2) cause a serious autosomal dominant inherited movement disorder termed spinocerebellar ataxias type 11 (SCA11) [1, 2]. SCA11 is characterised by progressive cerebellar ataxia, pyramidal features, peripheral neuropathy, and on occasion dystonia, with age of onset from the early teens to the mid 20s [3]. TTBK2 is closely related to a neuronal specific protein kinase termed TTBK1, which was discovered in 1995 as a protein kinase in bovine brain extract that phosphorylated tau and tubulin [4]. TTBK2 consists of 1244 residues and apart from an N-terminal serine/threonine protein kinase domain (residues 20 to 280) possesses no distinctive functional domains or motifs.

Thus far, four distinct SCA11 families have been identified, each possessing a mutation leading to premature termination of the TTBK2 protein at around residue 450. This leaves the kinase catalytic domain intact, but eliminates most of the non-catalytic portion of the enzyme (Fig 1A). One of the affected families from Devon, UK, stretches over eight generations (family 1 in Fig 1A) [1]. All affected individuals of this family displayed progressive cerebellar ataxia, abnormal eye signs and pyramidal features, as well as cerebellar atrophy visible upon magnetic resonance imaging [1]. Neuropathological examination of the brain blocks of one affected family-1 individual, revealed gross atrophy of the cerebellum accompanied by severe and near-complete loss of Purkinje cells, with a marked preservation of the basket cells, and a significant loss of cerebellar granule cells [1]. There were also changes consistent with pathological aging, with some tangles and β -amyloid-positive plaques observed in the neocortex, hippocampus, transentorhinal, entorhinal and insular cortex [1].

TTBK2 belongs to the casein kinase CK1 group of eukaryotic protein kinases composed of CK1 isoforms (CK1 α , CK1 α 2, CK1 δ , CK1 ϵ , CK1 γ 1, CK1 γ 2, CK1 γ 3), Vaccinia Related Kinase (VRK) isoforms (VRK1, VRK2 and VRK3) and TTBK isoforms (TTBK1 and TTBK2) [5]. CK1 differs from most other protein kinases by the presence of the sequence S-I-N motif instead of A-P-E in kinase domain region VIII [6]. TTBK1 and TTBK2 possess a P-P-E motif at this site. TTBK2 possesses 38% identity with CK1 δ within the kinase domain, but there is no obvious homology beyond the catalytic moiety of TTBK to CK1 or VRK isoforms. TTBK1 and TTBK2 share 84% identity within the catalytic domain and also display significant homology in the non-catalytic region.

TTBK isoforms have been found in many species including, mouse, zebrafish, *C.elegans* and *Drosophila* [7]. TTBK1 is mainly expressed in neuronal tissues [8], whereas TTBK2 is more widely expressed and has been observed in tissues including heart, muscle, liver, thymus, spleen, lung, kidney, testis and ovary [9, 10]. In situ hybridization showed that TTBK2 mRNA was present in all brain regions in human, rat and mouse tissue [1]. Highest expression of TTBK2 mRNA was observed in the cerebellum Purkinje cells, granular cell layer, hippocampus, midbrain and substantia nigra [1]. Lower expression was seen in the cortex of human, rat and mouse brains [1].

Biochemical investigations initially identified a proteolytic fragment of the catalytic domain of TTBK2 encompassing residues 1-316, in various brain extracts that was capable of phosphorylating tau at two sites (Ser208 and Ser210) [9, 10]. Phosphorylation of these residues primes Tau for the phosphorylation by isoforms of Glycogen Synthase Kinase-3, an enzyme that has also been suggested to modulate tau pathology [11]. TTBK1 was reported to phosphorylate tau at four residues (Ser198, Ser199, Ser202 and Ser422) [8]. More recently overexpression of TTBK1 in mouse, was reported to enhance phosphorylation and oligomerisation of tau in the brain [12]. Whether endogenous TTBK1 and/or TTBK2 regulate phosphorylation of endogenous

tau has not been established. Recent genetic studies have also implicated TTBK1 in Alzheimer's disease and in tangle formation [13, 14]. Thus far only one brain from a SCA11 family-1 patient has thus far been analysed and it displayed some tau deposition [1]. This may suggest that TTBK2 could be involved in regulating tau, but much further investigation is required to substantiate this conclusion.

Despite this previous work, little is understood about TTBK2 substrate specificity and how SCA11 truncating mutations impact on protein expression, kinase activity, stability and localisation. We have therefore undertaken an initial analysis of TTBK2 substrate specificity and shown that it has a conspicuous preference for a phosphotyrosine at the +2 position relative to the phosphorylation site. We exploit this information to develop an optimised peptide substrate to assess TTBK2 catalytic activity. Furthermore, we demonstrate that SCA11 truncating mutations markedly enhance TTBK2 protein expression, lead to inhibition of TTBK2 kinase activity and promote nuclear localisation. We generate TTBK2 knock-in mice expressing an SCA11 disease causing mutation and confirm that this results in the inhibition of endogenous protein kinase activity. We find that in homozygosity the SCA11 mutation causes embryonic lethality. These findings will help with further investigations into the function and regulation of TTBK2 as well as its role in SCA11.

Materials and Methods

Reagents and general methods

Lysis Buffer contained 50 mM Tris/HCl, pH 7.5, 1 mM EGTA, 1 mM EDTA, 1 mM sodium orthovanadate, 10 mM sodium- β -glycerophosphate, 50 mM NaF, 5 mM sodium pyrophosphate, 0.27 M sucrose, 1 mM benzamidine and 2 mM phenylmethanesulphonylfluoride (PMSF), supplemented with either 1% (v/v) Triton X-100 or 0.5% (v/v) NP-40 and 150 mM NaCl as indicated. Buffer A contained 50 mM Tris/HCl, pH 7.5, 50 mM NaCl, 0.1 mM EGTA and 0.27 M sucrose. Tissue-culture reagents were from Life Technologies and [γ - 32 P]-ATP was from Perkin Elmer. P81 phosphocellulose paper was from Whatman. The Flp-in T-REx system was purchased from Invitrogen and stable cell lines were generated following the manufacturer instructions by selection with hygromycin.

The coding region of full length human TTBK2 was amplified by PCR from Image clone 4829013 (NCBI acc. BC071556) and subcloned as a *NotI-NotI* fragment into several expression vectors. Site directed mutagenesis was carried out using the QuickChange® method (Stratagene) with the KOD polymerase (Novagen) in the presence of DMSO. All DNA constructs were verified by DNA sequencing, which was performed by The Sequencing Service, School of Life Sciences, University of Dundee, Scotland, UK.

Antibodies

A fragment of the mouse TTBK2 fusion protein encompassing residues 314-385 with an N-terminal GST (glutathione S-transferase) tag was expressed in bacteria and purified by glutathione-Sepharose chromatography. After cleavage of the GST tag, TTBK2 (314-385) was used as an immunogen to raise a sheep polyclonal antibody (S572C). Antibodies were affinity purified from antisera using the TTBK2 314-385 protein immunogen. Anti GST antibody was raised in sheep against the GST protein (S902A, 1st bleed). Anti GFP (green fluorescent protein) antibody (S268B) was raised in sheep against recombinant GFP protein and affinity-purified against the antigen. Secondary antibodies coupled to horseradish peroxidase were obtained from Thermo Scientific and fluorescent secondary antibodies employed for the Odyssey Infrared System were from Rockland.

Immunological procedures

Cell lysates (20-30 μ g) and immunoprecipitates were subjected to SDS-PAGE electrophoresis using 10% gels and transferred onto nitrocellulose membranes. Membranes were blocked for 20 minutes at room temperature in 10% (w/v) dried non-fat milk powder in TBS-T (Tris buffered saline with 1% Tween-20). All primary antibodies used for immunoblotting were used at 1 μ g/ml in 5% milk in TBS-T. Secondary antibodies used were either horseradish peroxidase-conjugated or fluorescent antibodies. For immunoprecipitations, TTBK2 antibody was covalently coupled to protein G-Sepharose beads at a ratio of 1 μ g antibody/ μ l of beads using a dimethyl pimelimidate (DMP) procedure, or GFP-antibody coupled beads were used. The indicated amount of cell lysates were immunoprecipitated using 5 μ l bead volume of coupled antibody for 1 hour, washed twice with lysis buffer containing 0.5 M NaCl and twice with Buffer A. Immunoprecipitates were either subjected to protein kinase activity as described below or to immunoblot analysis.

TTBK2 immunoprecipitation kinase assays

Peptide kinase assays were set up in a total volume of 50 μ l in 50 mM Tris pH 7.5, 0.1 mM EGTA, 10 mM MgCl₂ and 0.1 mM γ - 32 P-ATP (~500-1000 cpm/pmol) in the presence of the indicated concentration of peptide substrate. The assays were performed for 20 minutes at 30 °C. When purified proteins were used, reactions were terminated by applying 40 μ l of the reaction mixture on to P81 phosphocellulose paper. In the case of immunoprecipitated TTBK2, reactions were terminated by adding 10 μ l of 0.2M EDTA and gentle mixing. After a short spin, 50 μ l of the

reaction was spotted onto P81 phosphocellulose paper. After extensive washing in 50 mM phosphoric acid, reaction products were quantified by Cerenkov counting. Km and Vmax parameters were calculated using the Michaelis-Menten model of non-linear regression with the GraphPad Prism V5 program.

Fluorescence microscopy

HEK293 Flp-in T-REx stable cell lines harbouring GFP-tagged wild-type and mutant forms of TTBK2 were generated using standard protocols. Cells were grown on coverslips and induced with 0.1 $\mu\text{g/ml}$ doxycycline for 16 hours. Cells were fixed for 10 minutes with 4% paraformaldehyde at room temperature and washed twice for 5 minutes. After permeabilisation in phosphate-buffered saline (PBS) containing 1% Triton-X (v/v) for 10 minutes at room temperature, cells were incubated for 10 minutes with donkey serum (Sigma D9663) and then for 1 hour with 0.5 $\mu\text{g/ml}$ of anti-TTBK2 antibody. Cells were washed 3 times with PBS and incubated 30 minutes with the secondary antibody (Alexa Fluor 594) diluted 1:500 in PBS. After three further washes with PBS, cells were incubated with DAPI (4',6-diamino-2-phenylindole) for 10 minutes and mounted onto slides using Hydromount (National Diagnostics). Images were collected on a Zeiss LSM 700 confocal microscope using an α Plan-Apochromat x100 objective.

Quantitation of GFP-TTBK2 localisation

GFP expressing cell lines were fixed and stained with DAPI to identify their nuclei. Fields of cells selected on the basis of the DAPI staining were chosen at random and single optical sections through the nucleus and cytoplasm in the DAPI and GFP channels were collected sequentially on the Zeiss LSM 700 confocal microscope using the alpha Plan-Apochromat 100x objective. These images were quantified using the image-processing software Velocity (Perkin-Elmer). The nuclei were identified using the DAPI channel and the average GFP nuclear intensity measured for each cell. The whole cells including the nuclei were identified from the GFP channel and the area of the previously identified nuclei removed from these areas. The average intensity in the remaining cytoplasm was then measured for each cell. The nuclear intensity was then expressed as a ratio of the cytoplasmic intensity in order to avoid variability in protein expression by the cells. For each cell lines between 260 and 460 cells were counted over 10 fields of cells.

Animals and the generation of TTBK2 knock-in mouse

Animal studies were approved by the University of Dundee Ethics Committee and performed under a UK Home Office project license. Animals were obtained from Harlan Ltd (UK) and Taconic Artemis pharmaceuticals and maintained under specific pathogen-free conditions. The knock-in mice were generated by Taconic Artemis on an inbred C57BL/6J background as described in Figure 5. Genotyping was performed by PCR on DNA extracted from ears or embryonic membranes. Primers 1 (5'-CATTGTTGGCATTATTTCAAAGG-3') and 2 (5'-AGTAGTAGTAGTAGTAGTAACATGG-3') were used to detect the wild-type and knock-in alleles. The PCR program consisted of 2 min at 95°C, 15 sec at 95°C, 30 sec at 60°C, and 10 sec at 72°C for 35 cycles.

Embryos and mouse embryonic fibroblasts culture

To generate embryos, TTBK2 heterozygous mice were crossed and embryonic development was estimated considering the day of vaginal plug observation as 0.5 dpc. Pregnant females were sacrificed and uterine horns were collected in PBS. The embryos were dissected from the decidua in M2 media (Sigma M7167) at room temperature and fixed in 4 % PFA for 2 hours and washed and stored in PBS for phenotypic analysis. Mouse embryonic fibroblasts were generated from embryos at 9.5 to 10.5 dpc. Embryos were removed from M2 media and placed in trypsin for 10 minutes at 37°C. From this stage, embryos were cultured in advanced DMEM/F12 media (Invitrogen 12634) supplemented with 10% FBS, 1X MEM non-essential amino acids, 2 mM L-glutamine and 0.1 mM 2-mercaptoethanol.

Results

Analysis of substrate specificity of TTBK2 by positional scanning peptide library approach

We initially utilised the positional scanning peptide library approach [15, 16] to probe the substrate specificity preferences of TTBK2. This assay employs 198 biotinylated peptide libraries that each contain a 1:1 mixture of serine and threonine at the central position and one additional position fixed to one of the 20 amino acids, as well as phosphothreonine, or phosphotyrosine. Phosphothreonine and phosphotyrosine were included to allow substrate specificity analysis of kinases such as CK1 to which TTBK2 is related that have preferences for priming phosphorylation sites. All other positions contain an equimolar degenerate mixture of natural amino acids (except serine, threonine, and cysteine). We screened the 198 libraries using γ - ^{32}P -ATP and recombinant TTBK2(1-450) or kinase inactive TTBK2[D163A](residues 1-450) expressed in HEK293 cells. Biotinylated peptides were then captured on a streptavidin-coated membrane. The relative amino acid preference at each position was determined by quantifying ^{32}P -radioactivity incorporation following phospho-imaging. The key striking preference observed from this analysis was for a phosphotyrosine residue at the +2 position downstream from the site of phosphorylation (Fig 1B). For experiments undertaken with the kinase-inactive TTBK2[D163A], vastly lower overall levels of phosphorylation were observed with no preference for a +2 phosphotyrosine.

Elaboration of TTBKtide as an optimal peptide substrate

As TTBK2 is a member of the CK1 family we decided to verify whether TTBK2 would phosphorylate a model peptide substrate termed CK1tide that is frequently employed to assess CK1 isoform activity [17]. CK1 δ phosphorylates CK1tide (RRKDLHDDEEDEAMS*ITA) at the Ser residue marked with an asterisk [17], and we confirmed that TTBK2[1-450] also phosphorylates CK1tide specifically at this Ser residue (Fig S1). We next investigated the effects of introducing a phosphotyrosine residue at every position from the -5 to the +4 residue. This confirmed the findings of the positional scanning peptide library approach, revealing that introducing a phosphotyrosine residue at the +2 position, but not at any other position, strongly promoted peptide phosphorylation, principally by decreasing the K_m approximately 8-fold (Fig 1C & D). The CK1tide peptide with a phosphotyrosine residue at the +2 position was named TTBKtide (RRKDLHDDEEDEAMSIYpA). Introducing a phosphothreonine rather than a phosphotyrosine at the +2 position failed to enhance peptide phosphorylation (Fig 1D). Substituting the phosphorylated Ser residue in TTBKtide for a Thr did not effect phosphorylation by TTBK2, but substitution with a Tyr residue abolished phosphorylation (Fig 1D).

Molecular basis for phosphate-priming

CK1 isoforms possess a well-known requirement for priming phosphorylation [18-20]. The crystal structure of yeast CK1 [21] and human CK1 δ [22] reveals the presence of a sulfate-binding groove on the small lobe of the kinase domain, predicted to function as the phosphate-priming site (Fig 2A). Four highly conserved basic Lys/Arg residues on CK1 isoforms form ionic interactions with the sulfate residue (Fig 2A). Three of these residues are conserved in TTBK1 and TTBK2 (Lys50, Lys143 and Arg181). The fourth residue is an Ala in TTBK2 (Ala184) as well as in TTBK1 (Fig 2B). To verify whether these residues on TTBK2 could be involved in enhancing phosphorylation of +2 phosphotyrosine containing substrates, we studied the effect that mutation of Lys50, Lys143, Arg181 and Ala184 had on the phosphorylation of TTBKtide. Mutation of Lys50 or Lys143 to either Glu or Ala inactivated/destabilised TTBK2 (SFig 2A) and equivalent mutations in CK1 δ had similar effects (SFig 2B). In contrast, mutation of Arg181 or Ala184 did not affect stability (Fig 2C) or the intrinsic TTBK2 kinase activity as judged by the ability of these mutants to phosphorylate a peptide lacking the +2 phosphotyrosine residue (Fig 2D). However, the ability of TTBK2[Arg181Ala or Glu] or TTBK2[Ala184Gly] or

Glu] mutants to phosphorylate tyrosine-phosphorylated TTBKtide was markedly impaired (Km values 100-150 μ M compared to 18 μ M for wild-type TTBK2) (Fig 2D). This data suggests that TTBK2 possesses a phosphate-priming groove similar to CK1, except that it is involved in recognising +2 phosphotyrosine residues rather than N-terminal phosphoserine/phosphothreonine.

Disease causing TTBK2 mutations markedly increase protein expression and inhibit kinase activity

We next investigated how disease-causing truncation mutations affect TTBK2 protein expression as well as kinase activity. We generated HEK293 cells that stably express GFP-tagged versions of full-length TTBK2, family-1 and family-2 disease variants of TTBK2 (see Fig 1) as well as a TTBK2[1-450] truncation mutant. We observed that both family-1 and family-2 mutations and residue 450-truncation mutants were expressed at higher levels than full-length wild-type or kinase-inactive GFP-TTBK2[D163A] (Fig 3A). Similarly, we also observed increased expression of the truncation mutants of TTBK2 possessing FLAG (SFig 3A) or GST (SFig 3B) tags.

Monitoring the rate of degradation following pulse labelling of cells with 35 S-methionine revealed that both wild-type and disease mutant family-1 TTBK2 displayed a similar ~24 h half-life in HEK293 cells, indicating that there was not a significant difference in the rate at which these proteins are degraded in cells (SFig 4).

We next immunoprecipitated GFP-TTBK2 variants and quantified their intrinsic activity employing the TTBKtide peptide substrate. We calculated specific activity of wild-type and mutant forms of TTBK2 by normalising for differences in protein expression using quantitative LICOR immunoblot analysis. This revealed that full-length wild-type TTBK2 possessed approximately 10-fold higher specific activity than the family-1 and family-2 disease mutants or the TTBK2(1-450) mutant (Fig 3A). The kinase-inactive full-length TTBK2[D163A] or truncated TTBK2[D163A](1-450) displayed no detectable activity, establishing that activity of TTBK2, rather than that of a contaminating kinase is being measured (Fig 3A). Similar analysis of the specific activity of wild-type and mutants of TTBK2 variants with FLAG (SFig 3A) or GST (SFig 3B) epitope tags confirmed that SCA11 truncating mutations markedly suppressed kinase activity.

Disease causing TTBK2 mutations promote nuclear localisation

We analysed the cellular localisation of stably expressed variants of GFP-TTBK2 in HEK293 cells. This revealed that full-length wild-type TTBK2 (Fig 4, panel 1) or full-length, kinase-inactive TTBK2[D163A] (Fig 4, panel 2) was expressed at higher levels in the cytosol than the nucleus. However, TTBK2(family-1 mutation) (Fig 4, panel 3) or truncated TTBK2(1-450) (Fig 4, panel 4&5) were expressed at similar levels in both the cytosol and the nucleus. Quantitation of the ratio's of nuclear versus cytosolic TTBK2, establishes that ~2-fold higher proportion of TTBK2 (family-1 mutation) and truncated TTBK2(1-450) is localised in the nucleus compared to full length TTBK2 (Fig 4, panel 7).

Generation of TTBK2 (family-1 mutation) knock-in mice

Knock-in mice which precisely mimic the one-base insertion of adenosine in exon-13 at nucleotide 1329, observed in SCA11 family-1 [1], were generated as described in Figure 5. We observed that heterozygous TTBK2^{fmly1/+} mice were viable and fertile. The oldest TTBK2^{fmly1/+} mice we have thus far analysed are ~1 year of age and display no overt phenotype. Anatomical dissection of 1-year-old mice brains also revealed no discernable abnormality. Breeding of heterozygous TTBK2^{fmly1/+} mice resulted in no homozygous TTBK2^{fmly1/fmly1} mice being born (Fig 6A), indicating that the homozygous mutation resulted in embryonic lethality. We therefore dissected embryos at different stages of development and found that at E10-TTBK2^{fmly1/fmly1} embryos were detected at the expected Mendelian frequency but displayed major abnormalities compared to littermate TTBK2^{fmly1/+} or TTBK2^{+/+} embryos. By stage

E11 no homozygous $TTBK2^{fmy1/fmy1}$ embryos were observed, suggesting that these embryos perished before this stage. Homozygous E10- $TTBK2^{fmy1/fmy1}$ embryos were developmentally delayed, lacking prominent sub-divisions of the developing brain and were smaller than wild-type littermates (Figure 6B). These embryos failed to complete embryonic turning movements or undergo normal caudal extension of the body; in several cases the rudimentary caudal body, which contained some somites (future vertebrae, muscle and dermis) and spinal cord, remained folded back on more rostral tissues (Figure 6B). This distortion and under-development of the main body axis (Figure 6B) are the likely causes of embryonic lethality.

Expression and activity of mutant TTBK2 in tissues and fibroblasts derived from knock-in mice

We next analysed endogenous TTBK2 expression and activity in various mouse tissues. This revealed significantly higher levels of TTBK2 protein and activity in brain and testes than other tissues investigated (Fig 7A). In wild-type $TTBK2^{+/+}$ brain and testes, TTBK2 migrated on an SDS polyacrylamide gel at the expected ~150 kDa size. As predicted, in tissues of the heterozygous $TTBK2^{fmy1/+}$ mice the level of full-length TTBK2 is reduced by ~50% and a truncated form of TTBK2 migrating at ~50 kDa that is not seen in the wild-type mice is observed (Fig 7B). We also analysed endogenous TTBK2 catalytic activity after immunoprecipitation from brain and testes extracts and found that TTBK2 activity was reduced ~40 to 50% in tissues derived from heterozygous $TTBK2^{fmy1/+}$ compared to wild-type littermate animals, consistent with the truncating mutation suppressing TTBK2 catalytic activity (Fig 7B).

We also analysed TTBK2 activity in mouse embryonic fibroblasts derived from wild-type $TTBK2^{+/+}$, heterozygous $TTBK2^{fmy1/+}$ and homozygous $TTBK2^{fmy1/fmy1}$ littermate stage E10 embryos. TTBK2 activity derived from homozygous $TTBK2^{fmy1/fmy1}$ cells was ~90% lower than activity observed in wild-type $TTBK2^{+/+}$ fibroblasts (Fig 7C). The heterozygous $TTBK2^{fmy1/+}$ displayed intermediate TTBK2 activity.

Discussion

We have undertaken the first characterisation of TTBK2 catalytic activity and substrate specificity, and we find that it possesses a marked preference for a phosphotyrosine residue at the + 2 position from the site of phosphorylation (Fig 1). Sequence comparisons indicate that TTBK2 possesses a phosphate-priming binding site in its catalytic domain equivalent to that in related CK1 isoforms. We find that mutating two key conserved residues within this putative phosphate-binding groove (Arg181 or Ala184) did not affect the ability of TTBK2 to phosphorylate a non-tyrosine phosphorylated peptide, but inhibited phosphorylation of a tyrosine phosphorylated peptide (Fig 2). The residues making up this putative phosphate-binding pocket are conserved on TTBK1 suggesting this isoform may also possess a preference for +2 residue phosphotyrosine priming. The key difference in the putative phosphate-binding groove between CK1 and TTBK1/TTBK2 is the presence of a non-basic Ala residue in TTBK1 and TTBK2 rather than a basic Lys in all CK1 isoforms. It would be interesting to explore whether this contributes towards the preference of TTBK2 for phosphotyrosine rather than phosphoserine/phosphothreonine priming in CK1 isoforms.

One of the most studied consensus phosphorylation site for CK1 isoforms is S/Tp-X-X-S/T, where S/Tp refers to a phospho-serine or phospho-threonine, X refers to any amino acid, and the underlined residues refer to the target site [18-20]. In the case of CK1, the priming phosphorylation site is at the -3 position rather than at the + 2 position for TTBK2. If both TTBK2 and CK1 use a similar phosphate-binding site within their catalytic domain, there would need to be marked differences in the mechanism and orientation at which primed phosphorylated substrates interact with CK1 and TTBK2. In future work it would be interesting to co-crystallise the catalytic domain of TTBK2 with a +2 tyrosine phosphorylated peptide to define the molecular mechanism by which TTBK2 interacts with such substrates and establish whether this putative phosphate binding groove we have analysed is involved. To our knowledge the structure of CK1 bound to an S/Tp-X-X-S/T motif containing peptide has not been reported, but would be of interest to compare with that of TTBK2. It would also be important to mine phosphorylation site databases for proteins phosphorylated on Sp/Tp-X-Yp motifs and determine whether any of these proteins might comprise physiological substrates for TTBK2.

Our analysis has enabled us to elaborate a reasonable peptide substrate for assessing TTBK2 activity (TTBK₂ide-RRKDLHDDEEDEAMSIYpA) that is phosphorylated with a K_m 18 μ M and a V_{max} of 76 U/mg. We have used this assay to investigate how SCA11 truncating mutations impact on TTBK2 activity and demonstrated that two familial SCA11 mutations analysed, induce ~10-fold reduction in TTBK2 protein kinase activity. Truncation of TTBK2 at residue 450 in close proximity to where the familial TTBK2 truncating mutations occurs, similarly suppressed TTBK2 activity. The observation that TTBK2 immunoprecipitated from TTBK2^{fmy1/+} mice possessed ~40% less activity (Fig 7B) and TTBK2 immunoprecipitated from TTBK2^{fmy1/fmy1} MEFs (Fig 7C) had ~10-fold lower activity, also supports the notion that SCA11 mutations drastically reduce endogenous TTBK2 activity. Thus these findings indicate that loss of TTBK2 activity could underpin development of SCA11 in patients.

It would be important to study in more detail the mechanism by which the SCA11-truncating mutations lead to suppression of TTBK2 protein kinase activity. The SCA11 truncating mutations leave the kinase catalytic domain intact removing a C-terminal non-catalytic region possessing no obvious functional domains (Fig 1A). The removal of the C-terminal non-catalytic region of TTBK2 might delete a motif required for kinase activation, activity or proper folding of the catalytic domain. Depending upon the mechanism by which SCA11 mutations suppress TTBK2 catalytic activity, it may be worth undertaking a drug screen to determine if it is

possible to identify compounds that could lead to the re-activation of truncated TTBK2 mutants. Such compounds could have potential for treating patients with SCA11.

The truncated TTBK2 mutants were expressed in HEK293 cells at significantly higher levels than the full-length wild-type enzyme (Fig 3 and Supplementary Fig 3). However, in the testes and brain of TTBK2^{fmyl1/+} mice, more similar levels of expression of the endogenous truncated and full-length forms of TTBK2 were observed (Fig 6). Although the relative expression of full-length and truncated mutants of TTBK2 in patients with SCA11 mutations has not yet been investigated, TTBK2 mRNA levels from lymphoblasts of affected individuals were significantly lower compared to lymphoblast mRNA from unaffected individuals [1]. This suggests that the premature stop codon in the TTBK2 mRNA, leads to nonsense-mediated decay of mutated mRNA. It is still likely that some of the truncated SCA11 protein is expressed in SCA11 patients as the mutant transcript was still detected [1]. Treating lymphoblasts from SCA11 affected individuals with cycloheximide an inhibitor of nonsense-mediated decay, increased TTBK2 mRNA to levels that are similar in the normal transcript [1]. Taking this data into consideration it is therefore possible that the truncated TTBK2 protein is indeed expressed at much higher levels than the full-length protein, but due to nonsense-mediated decay, less of the truncated protein is produced. This could account for why in the TTBK2^{fmyl1/+} mice, similar levels of wild type and truncated mutant protein are observed. In future work it would be important to analyse the relative levels of wild type and mutant TTBK2 mRNA in TTBK2^{fmyl1/+} mice. We also detected enhanced nuclear localisation of the truncated forms of TTBK2, indicating that inappropriate localisation within the nucleus could potentially contribute to the mechanism by which mutations in TTBK2 lead to SCA11. Potentially, the truncated TTBK2 mutants result in the inappropriate phosphorylation of nuclear proteins.

The developmental delay and small size of homozygous TTBK2^{fmyl1/fmyl1} embryos are consistent with a role for TTBK2 activity in the regulation of fundamental cellular processes, such as cell proliferation. The failure of embryonic turning and under development of the body axis might also lead to a poor placental connection and hence embryonic lethality. TTKB1 expression is prominently localised in cortical and hippocampal neurons [8]. Further insight into the TTKB2 phenotype and its role in spinocerebellar ataxia would be gained by establishing its expression pattern, particularly with respect to its localisation in the cerebellum. The TTBK2^{fmyl1/+} mice as well as TTBK2^{fmyl1/fmyl1} MEFs will be useful in validation of potential TTBK2 substrates that are identified.

In conclusion, our study provides some initial insights into substrate specificity of TTBK2 and how SCA11 causing mutations impact on kinase activity and localisation. In future studies it would be important to define the substrates that TTBK2 phosphorylates and investigate whether reduced phosphorylation of these targets contributes to the development of SCA11. In particular, it would be interesting to determine whether physiological TTBK2 substrates were primed with a +2 phosphotyrosine and how regulation of tyrosine phosphorylation was coupled to the control of these TTBK2 targets. Identifying the key targets of TTBK2 could provide vital new insights into the molecular mechanism underpinning the development of spinocerebellar ataxia and result in new ideas as to how this debilitating disease might be better treated in the future.

Acknowledgements

We thank Gail Fraser for genotyping of the mice, the DNA Sequencing Service (School of Life Sciences, University of Dundee, Scotland) and the protein production and antibody purification teams [Division of Signal Transduction Therapy (DSTT), University of Dundee] coordinated by Hilary McLauchlan and James Hastie. NE is funded by an MRC-UK Studentship. EF is a PhD student supported by the Wellcome Trust and KGS is funded by an MRC programme grant G0600234. We thank the Medical Research Council, the European Regional Development Fund grant for an Innovation Pipeline for Translational Science (LUPS/ERDF/2008/2/1/0429) and the pharmaceutical companies supporting the Division of Signal Transduction Therapy Unit (AstraZeneca, Boehringer-Ingelheim, GlaxoSmithKline, Merck KgaA and Pfizer) for financial support.

Author Contributions

MB undertook most of the experiments shown in Fig 3, 4, 6 and 7. NE performed analysis of substrate specificity of TTBK2 (Fig 1 & 2 and helped with analysis of Fig 5). MG and LCC performed and analysed positional scanning peptide library experiments (Fig 1B). LG undertook initial studies on TTBK2. MD undertook cloning. AP undertook cellular localisation studies (Fig 4). EF & KGS undertook embryo dissection and analysis of embryonic development (Fig 6). MB, NE and DRA planned experiments and analysed the data. MB and DRA wrote the manuscript.

References

- 1 Houlden, H., Johnson, J., Gardner-Thorpe, C., Lashley, T., Hernandez, D., Worth, P., Singleton, A. B., Hilton, D. A., Holton, J., Revesz, T., Davis, M. B., Giunti, P. and Wood, N. W. (2007) Mutations in TTBK2, encoding a kinase implicated in tau phosphorylation, segregate with spinocerebellar ataxia type 11. *Nat Genet.* **39**, 1434-1436
- 2 Bauer, P., Stevanin, G., Beetz, C., Synofzik, M., Schmitz-Hubsch, T., Wullner, U., Berthier, E., Ollagnon-Roman, E., Riess, O., Forlani, S., Mundwiler, E., Durr, A., Schols, L. and Brice, A. (2010) Spinocerebellar ataxia type 11 (SCA11) is an uncommon cause of dominant ataxia among French and German kindreds. *J Neurol Neurosurg Psychiatry.* **81**, 1229-1232
- 3 Houlden, H. (2008) Spinocerebellar Ataxia Type 11. In *GeneReviews* (Pagon, ed.), University of Washington, Seattle
- 4 Takahashi, M., Tomizawa, K., Sato, K., Ohtake, A. and Omori, A. (1995) A novel tau-tubulin kinase from bovine brain. *FEBS Lett.* **372**, 59-64
- 5 Manning, G., Whyte, D. B., Martinez, R., Hunter, T. and Sudarsanam, S. (2002) The protein kinase complement of the human genome. *Science.* **298**, 1912-1934
- 6 Hanks, S. K. and Hunter, T. (1995) Protein kinases 6. The eukaryotic protein kinase superfamily: kinase (catalytic) domain structure and classification. *Faseb J.* **9**, 576-596
- 7 Manning, G., Plowman, G. D., Hunter, T. and Sudarsanam, S. (2002) Evolution of protein kinase signaling from yeast to man. *Trends Biochem Sci.* **27**, 514-520
- 8 Sato, S., Cerny, R. L., Buescher, J. L. and Ikezu, T. (2006) Tau-tubulin kinase 1 (TTBK1), a neuron-specific tau kinase candidate, is involved in tau phosphorylation and aggregation. *J Neurochem.* **98**, 1573-1584
- 9 Takahashi, M., Tomizawa, K., Ishiguro, K., Takamatsu, M., Fujita, S. C. and Imahori, K. (1995) Involvement of tau protein kinase I in paired helical filament-like phosphorylation of the juvenile tau in rat brain. *J Neurochem.* **64**, 1759-1768
- 10 Tomizawa, K., Omori, A., Ohtake, A., Sato, K. and Takahashi, M. (2001) Tau-tubulin kinase phosphorylates tau at Ser-208 and Ser-210, sites found in paired helical filament-tau. *FEBS Lett.* **492**, 221-227
- 11 Noble, W., Planel, E., Zehr, C., Olm, V., Meyerson, J., Suleman, F., Gaynor, K., Wang, L., LaFrancois, J., Feinstein, B., Burns, M., Krishnamurthy, P., Wen, Y., Bhat, R., Lewis, J., Dickson, D. and Duff, K. (2005) Inhibition of glycogen synthase kinase-3 by lithium correlates with reduced tauopathy and degeneration in vivo. *Proc Natl Acad Sci U S A.* **102**, 6990-6995
- 12 Xu, J., Sato, S., Okuyama, S., Swan, R. J., Jacobsen, M. T., Strunk, E. and Ikezu, T. (2010) Tau-tubulin kinase 1 enhances prefibrillar tau aggregation and motor neuron degeneration in P301L FTDP-17 tau-mutant mice. *FASEB J.* **24**, 2904-2915
- 13 Vazquez-Higuera, J. L., Martinez-Garcia, A., Sanchez-Juan, P., Rodriguez-Rodriguez, E., Mateo, I., Pozueta, A., Frank, A., Valdivieso, F., Berciano, J., Bullido, M. J. and Combarros, O. (2011) Genetic variations in tau-tubulin kinase-1 are linked to Alzheimer's disease in a Spanish case-control cohort. *Neurobiol Aging.* **32**, 550 e555-559
- 14 Yu, N. N., Yu, J. T., Xiao, J. T., Zhang, H. W., Lu, R. C., Jiang, H., Xing, Z. H. and Tan, L. (2011) Tau-tubulin kinase-1 gene variants are associated with Alzheimer's disease in Han Chinese. *Neurosci Lett.* **491**, 83-86

- 15 Hutti, J. E., Jarrell, E. T., Chang, J. D., Abbott, D. W., Storz, P., Toker, A., Cantley, L. C. and Turk, B. E. (2004) A rapid method for determining protein kinase phosphorylation specificity. *Nat Methods*. **1**, 27-29
- 16 Turk, B. E., Hutti, J. E. and Cantley, L. C. (2006) Determining protein kinase substrate specificity by parallel solution-phase assay of large numbers of peptide substrates. *Nat Protoc*. **1**, 375-379
- 17 Marin, O., Meggio, F. and Pinna, L. A. (1994) Design and synthesis of two new peptide substrates for the specific and sensitive monitoring of casein kinases-1 and -2. *Biochem Biophys Res Commun*. **198**, 898-905
- 18 Flotow, H., Graves, P. R., Wang, A. Q., Fiol, C. J., Roeske, R. W. and Roach, P. J. (1990) Phosphate groups as substrate determinants for casein kinase I action. *J Biol Chem*. **265**, 14264-14269
- 19 Flotow, H. and Roach, P. J. (1989) Synergistic phosphorylation of rabbit muscle glycogen synthase by cyclic AMP-dependent protein kinase and casein kinase I. Implications for hormonal regulation of glycogen synthase. *J Biol Chem*. **264**, 9126-9128
- 20 Nakielny, S., Campbell, D. G. and Cohen, P. (1991) The molecular mechanism by which adrenalin inhibits glycogen synthesis. *Eur J Biochem*. **199**, 713-722
- 21 Xu, R. M., Carmel, G., Sweet, R. M., Kuret, J. and Cheng, X. (1995) Crystal structure of casein kinase-1, a phosphate-directed protein kinase. *EMBO J*. **14**, 1015-1023
- 22 Longenecker, K. L., Roach, P. J. and Hurley, T. D. (1996) Three-dimensional structure of mammalian casein kinase I: molecular basis for phosphate recognition. *J Mol Biol*. **257**, 618-631

Accepted Manuscript

Figure Legends

Figure 1. Domain structure and substrate specificity of TTBK2

(A) Schematic representation of the domain structure of TTBK2 showing the location of the three reported SCA11 causing mutations. Numbering of residues corresponds to human TTBK2. (B) Recombinant HEK293 purified GST-TTBK2 (1-450) WT and catalytically inactive GST-TTBK2 (1-450) D163A were used to screen a positional scanning peptide library consisting of 189 biotinylated peptide libraries in individual kinase assays. Reaction products were bound to streptavidin-coated membrane and, after washing, phosphorylation was visualised by phospho-imaging. (C) Peptides with various positions of the phosphotyrosine residue from +4 to -5 relative to the phosphorylated serine residue were synthesised and analysed for their ability to phosphorylate GST-TTBK2 (1-450) WT purified from HEK293 cells. K_m and V_{max} values were derived by non-linear regression analysis as described in the Methods section. (D) Three TTBKtide variants with serine, threonine and tyrosine at the phospho-acceptor position and a TTBKtide variant with a phosphothreonine at the +2 position were synthesised and the kinetics of their phosphorylation by GST-TTBK2[1-450] was analysed. K_m and V_{max} values were derived by non-linear regression analysis. NP denotes that the peptide was phosphorylated too poorly to undertake accurate kinetic analysis.

Figure 2. Molecular basis for phosphate priming

(A) High resolution structure of CK1 delta protein showing the sulphate binding site on the C-lobe of the kinase domain predicted to function as the phosphate priming region [22]. Lysine 38 (site A), Lysine 130 (site B), Arginine 168 (site C) and Lysine 171 (site D) form ionic interactions with the sulphate residue and are shown in orange. (B) Sequence alignment of the indicated species of TTBK1, TTBK2 and CK1 family enzymes showing the sequence conservation of the sulphate-binding residues. (C) Coomassie-stained gel of the GST-TTBK2[1-450] truncated form of the indicated wild-type (WT) and mutant proteins expressed and purified from HEK293 cells. (D) The indicated GST-TTBK2[1-450] truncated forms expressed in (C) were tested for their ability to phosphorylate TTBKtide (RRKDLHDDEEDEAMSIY^PA) and a variant of TTBKtide (RRKDLHDDEEDEAMSIYA) where the tyrosine at the +2 position is not phosphorylated. K_m and V_{max} values were derived by non-linear regression analysis.

Figure 3: Truncated form of TTBK2 are less active but express at a higher levels than the full-length kinase

HEK293 cells were transiently transfected with the wild-type (WT) and indicated mutants of Flag-tagged (A & B) or GST-tagged (C & D) TTBK2. (A & C) Cells were lysed and subjected to immunoblotting with the anti-TTBK2 antibody and the other indicated antibodies. (B & D) TTBK2 was immunoprecipitated from 30 μ g of cell extract and subjected to kinase activity assay (upper panel) followed by immunoblot analysis (lower panel). TTBK2 kinase activity was quantified employing 30 μ M TTBKtide and specific activity was calculated by correcting the amount of phosphate incorporation for protein levels in the immunoprecipitate using quantitative immunoblot with the Odyssey system and is presented as cpm/absorbance units (cpm/LICOR Arbitrary Units). The data are the average for duplicate experiments that were repeated four separate times with similar results. Dotted lines indicates that blots were on separate gels.

Figure 4. SCA11 disease mutations promote TTBK2 nuclear localisation

HEK293 cells stably expressing the indicated forms of GFP-TTBK2 were treated with 1 μ g/ml tetracycline for 16 hours to induce the expression of TTBK2 (panels 1 to 6). Cells were fixed with 4% paraformaldehyde and stained with antibody recognising TTBK2 and with DAPI for nuclear staining. Fluorescent imaging was performed on a confocal microscope. Similar results were obtained in four independent experiments. Quantitation of nuclear versus cytoplasmic levels of TTBK2 (panel 7) was undertaken as described in the Materials and methods. For each cell lines between 260 and 460 cells were counted over 10 fields of cells.

Figure 5. Targeting strategy used to generate TTBK2 knock-in mutations

(A) Diagram describing the knock-in construct, the endogenous allele containing exon 13 and the targeted allele with the puromycin cassette removed by Flp recombinase. The grey rectangles represent TTBK2 exons. The grey and black triangles represent FRT and Lox P sites, respectively. The positions of the TTBK2 primers (P1 and P2) used for genotyping are represented as short black lines with arrowheads. (B) Genomic DNA purified from the targeted ES cells of the indicated genotypes was digested with either ScaI or AvrI and subjected to Southern analysis with the corresponding DNA probes (positions shown). In the case of the 5' probe, the wild-type allele produces a 9.8kb fragment while the conditional knockin allele generates a 7.3kb fragment. Similarly, the 3' probe detects a fragment of 23.8 kb from the wild-type allele and a 15.kb fragment from the conditional knockin allele.(C) Genomic DNA was PCR amplified with TTBK2 primers P1, P2. The wild-type allele (detected using P1 and P2) generates a 220 bp product while the knockin allele generates a 381 bp product.

Figure 6. Embryonic lethality and knock-in embryo description

(A) TTBK2^{fmly1/+} mice were mated and the progeny genotyped as described in the Methods. The number of mice obtained is indicated for each genotype. (B) Wild-type and homozygous TTBK2^{fmly1/fmly1} embryos at E10 were detected at the expected Mendelian frequency. Mutant embryos are smaller and developmentally delayed, lacking prominent sub-divisions of the brain (arrowheads on wild-type embryo). Incomplete embryonic turning movements may result in failure to extend the body axis. 27 separate E10 TTBK2^{fmly1/fmly1} embryos have been analysed and similar phenotypes were observed.

Figure 7. Study of TTBK2 in wild-type and TTBK2^{fmly1/+} knock-in mice

(A) The indicated tissue extracts were generated from wild-type mice. Extracts were immunoblotted for TTBK2 (lower panel) or TTBK2 was immunoprecipitated and subjected to TTBK2 kinase assay employing the TTBKtide peptide substrate. The data are the average for duplicate experiments that were repeated four separate times with similar results. (B) Brain and testes lysates were generated from TTBK2^{+/+} and TTBK2^{fmly1/+} mice and subjected to immunoblot or TTBK2 kinase assay analysis, as in (A). (C) Mouse embryonic fibroblasts (MEFs) were generated from TTBK2^{+/+}, TTBK2^{fmly1/+} and TTBK2^{fmly1/fmly1} E10 embryos as described in the Methods. TTBK2 activity was assessed following immunoprecipitation as in (A). Due to the low levels of TTBK2 protein expressed in MEFs and high antibody background in immunoprecipitates, we were unable to detect expression of TTBK2 by immunoblot analysis.

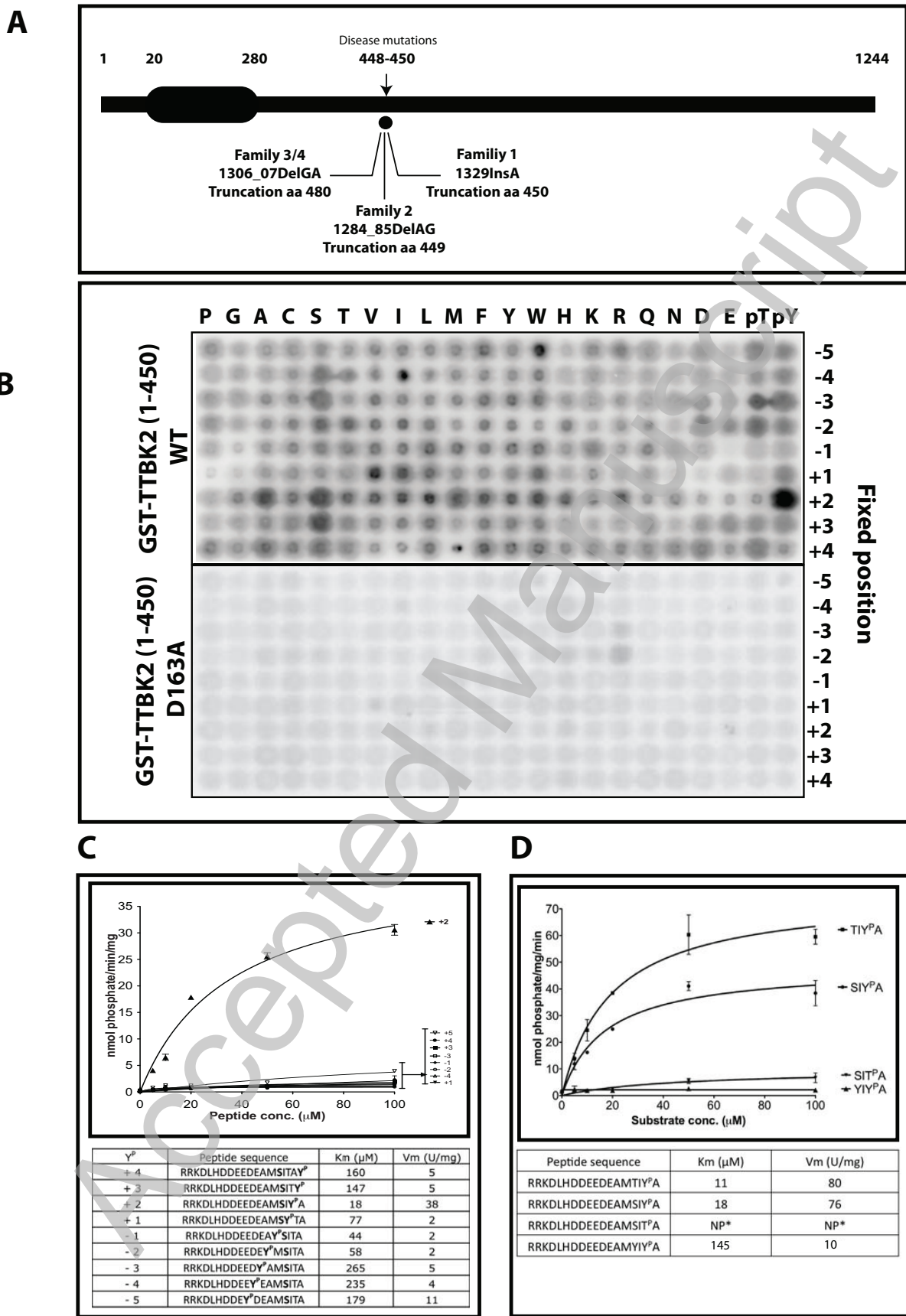


FIGURE 1

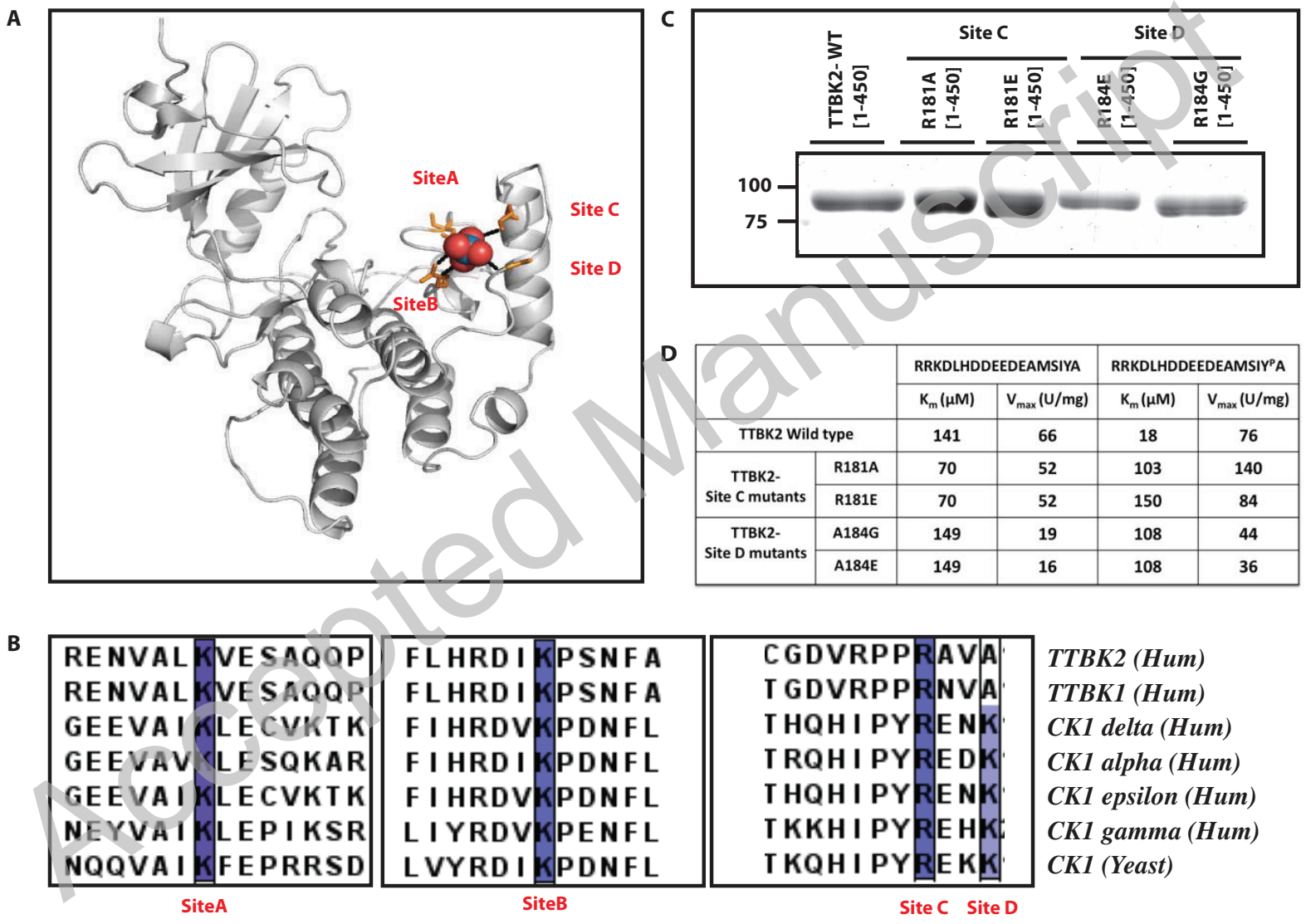


FIGURE 2

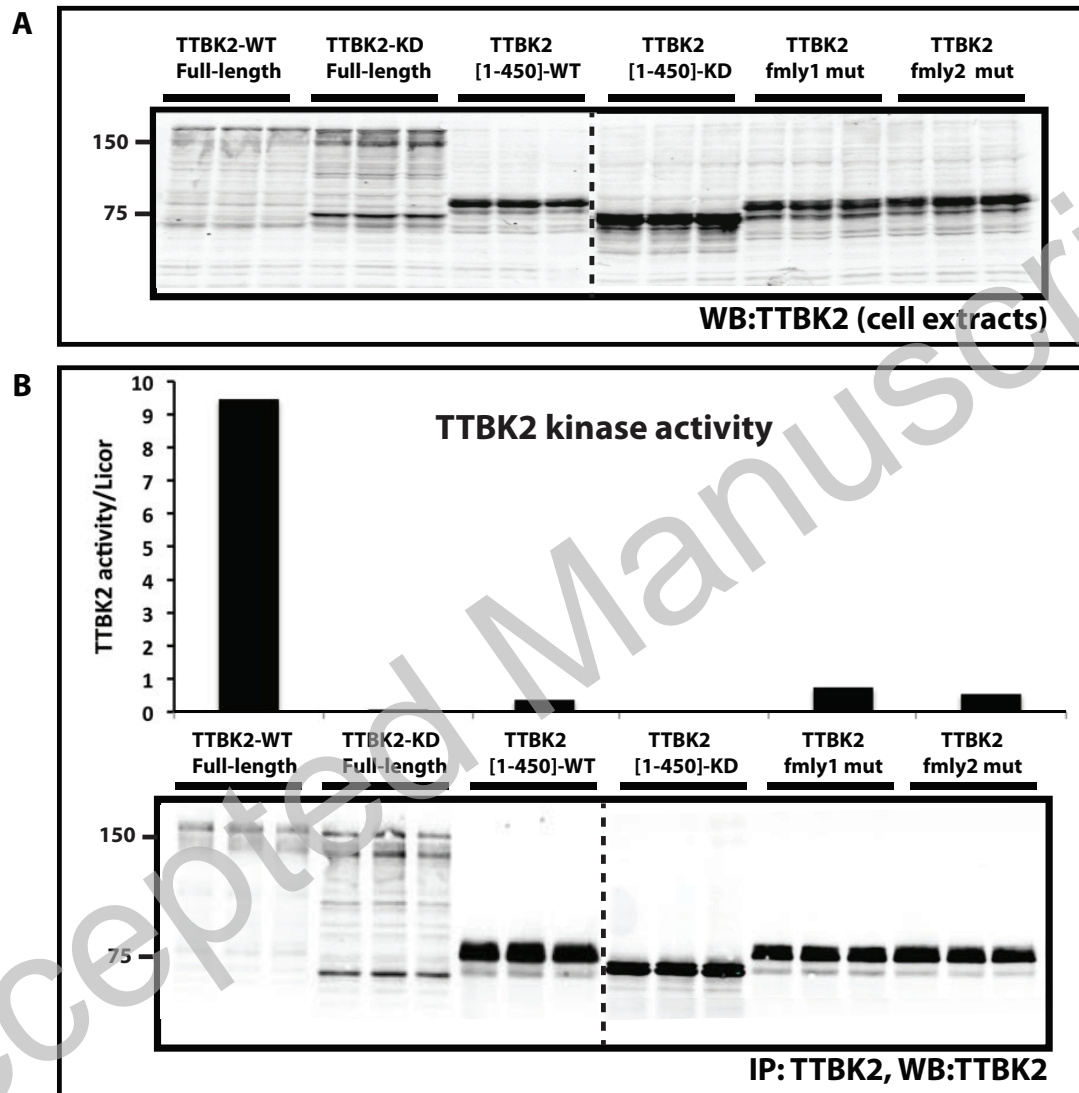


FIGURE 3

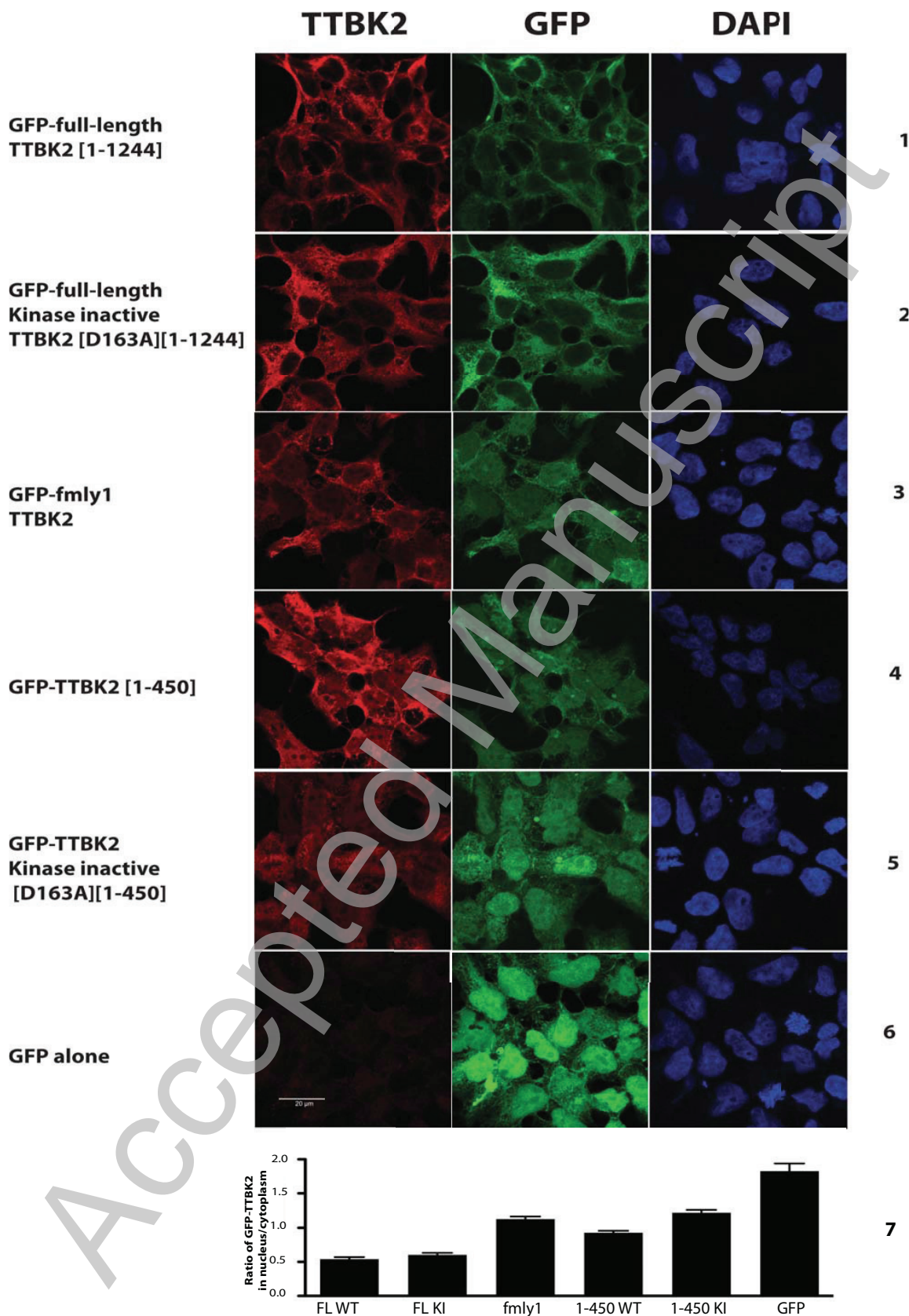


FIGURE 4

THIS IS NOT THE VERSION OF RECORD - see doi:10.1042/BJ20110276

THIS IS NOT THE VERSION OF RECORD - see doi:10.1042/BJ20110276

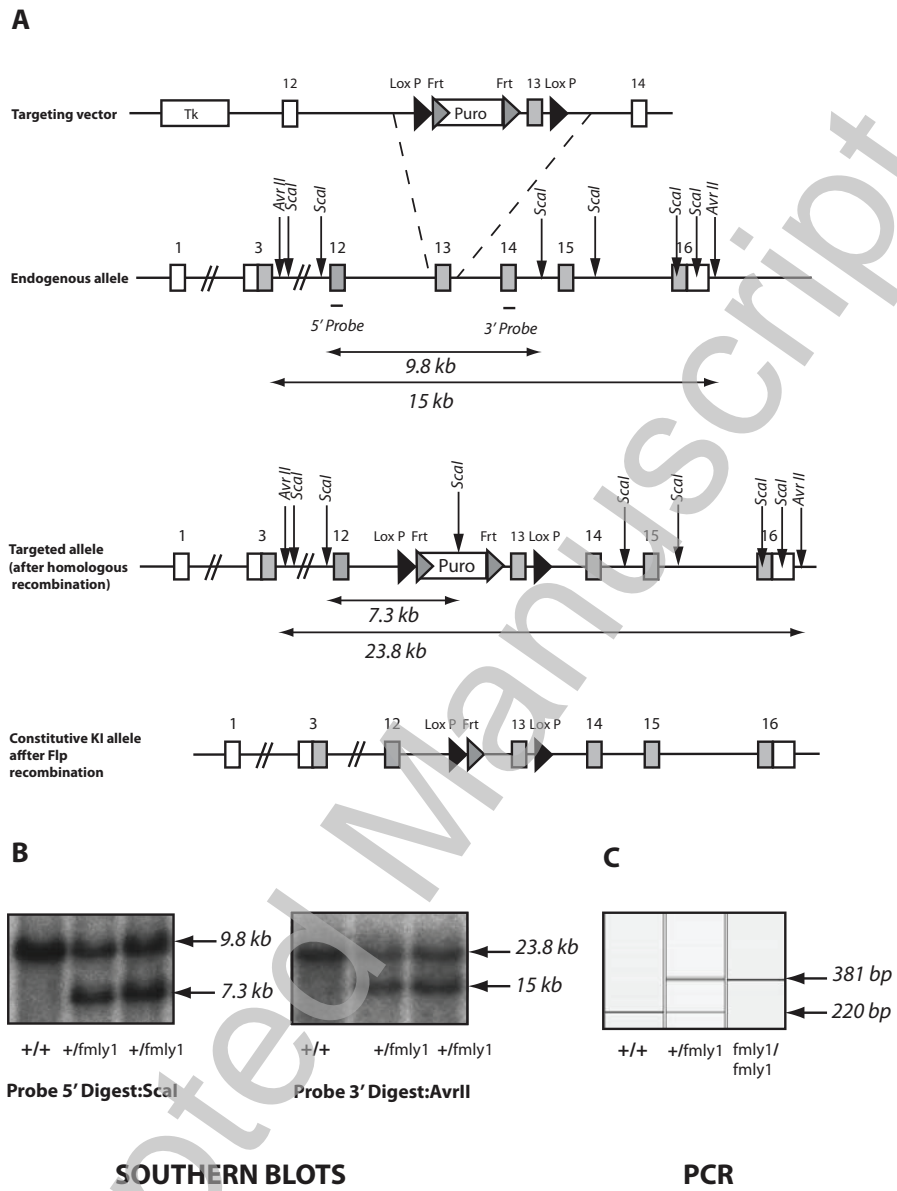
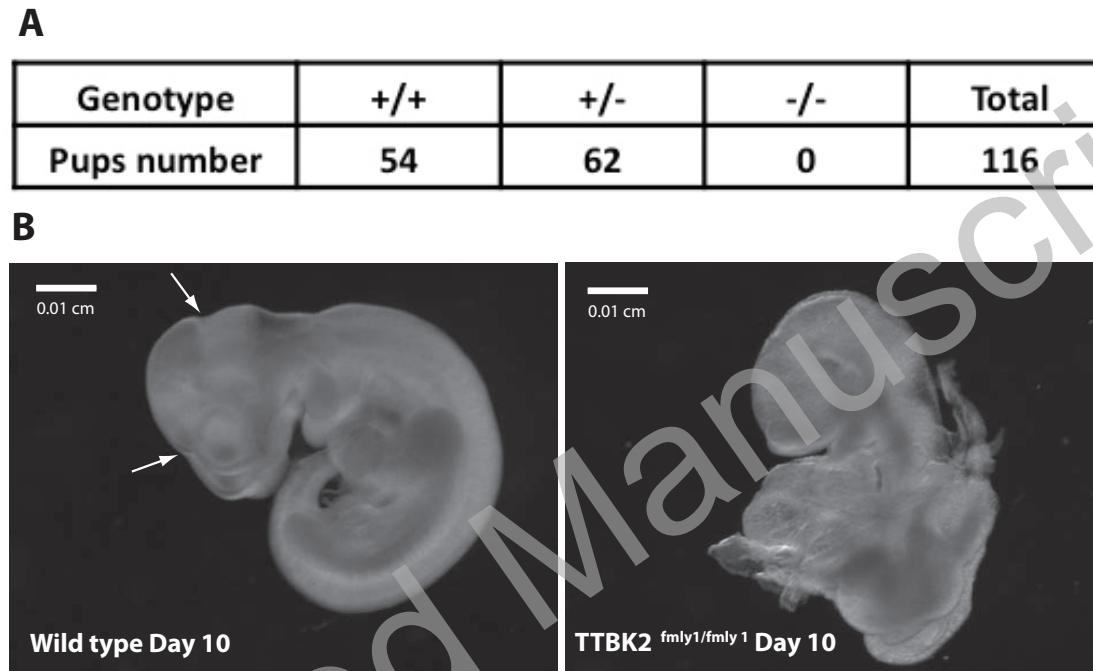


FIGURE 5

**FIGURE 6**

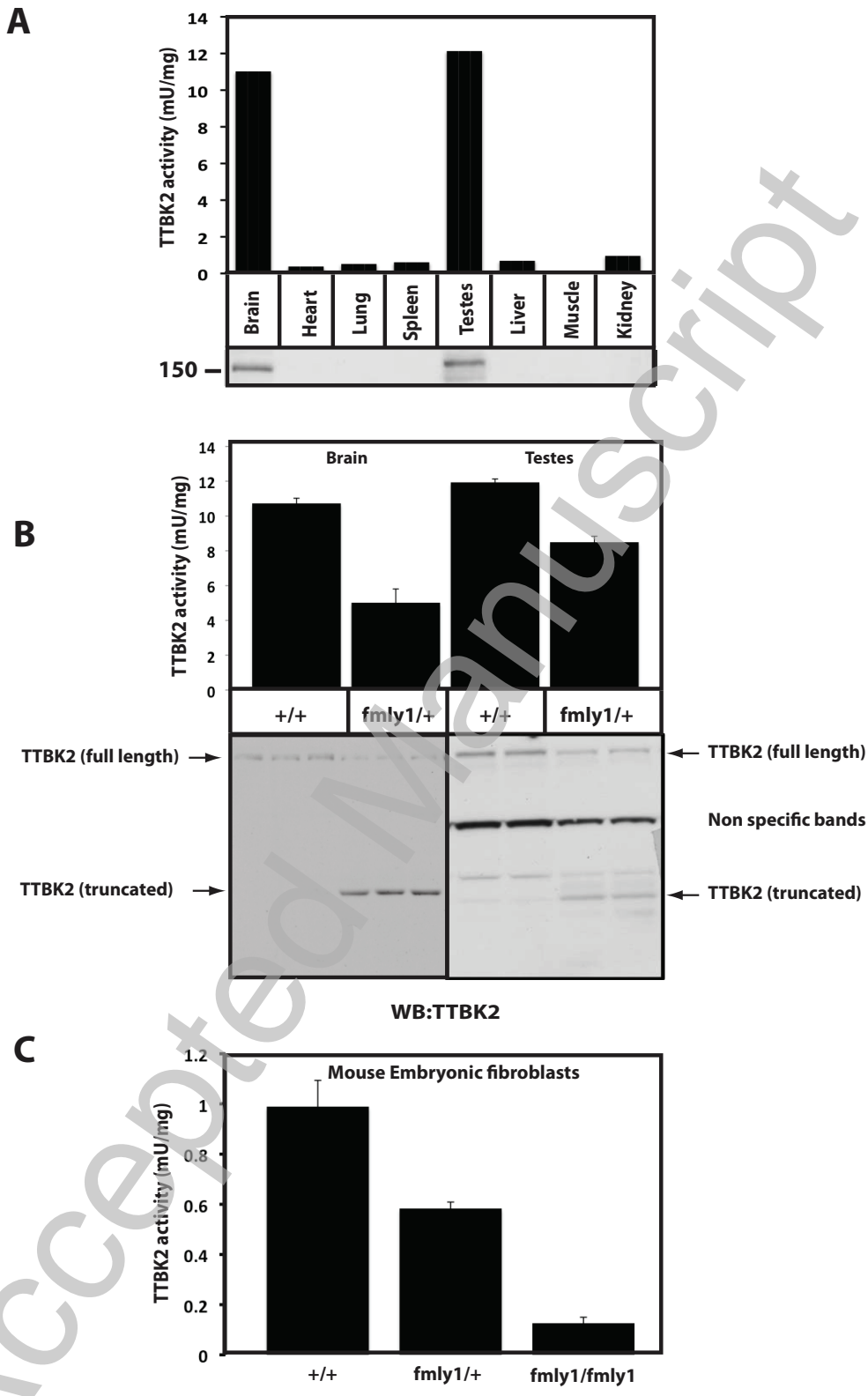


FIGURE 7